SYMPATHETIC PHENOMENA AS OBSERVED ON THE NOBEYAMA RADIOHELIOGRAPH

© 2025 V. E. Abramov-Maksimov

Main (Pulkovo) Astronomical Observatory of the Russian Academy of Sciences, St. Petersburg, Russia.

e-mail: beam@gaoran.ru

Received February 24, 2025

Revised April 06, 2025

Accepted June 17, 2025

Abstract. Sympathetic phenomena on the Sun are understood as events that occur with a small time interval in active regions that are distant from each other by significant distances. The presence of such phenomena indicates that even very distant active regions are physically connected with each other. In this paper we present the results of analyzing several sympathetic bursts detected from the analysis of the Nobeyama radioheliograph archive. The bursts in active regions distant from each other by distances from 400000 to1200000 km, occurred with a delay of 2 to 20 min. Estimates of the propagation velocity of the perturbing agent give a value of 1000-5000 km/sec.

DOI: 10.31857/S00167940250702e1

1. INTRODUCTION

Sympathetic phenomena on the Sun are active events (flares, bursts) occurring at short time intervals (e.g., a few minutes) in active regions (ARs) distant from each other by significant distances (up to10^6 км or more). The initiating flare is thought to trigger a secondary, initiating, flare with the help of some perturbing agent. A small time interval between events in AOs distant at a large distance from each other indicates a large propagation velocity of the disturbance. In addition to the term "sympathetic", some authors use the terms "simultaneous" and "synchronous" flares [Golubchina et al., 2004; Lebedev et al., 2025], considering sympathetic flares as a special case of simultaneous flares [Lebedev et al., 2025].

Sympathetic phenomena on the Sun were discovered in the 1930s from analyzing the statistics of optical flares [Richardson, 1936, 1951]. For a long time, the reality of these phenomena was questioned [Fritzova-Svestkova et al., 1976]. However, subsequent studies suggest that the phenomena are real (e.g., [Wang et al., 2001; Wheatland and Craig, 2006]). Various mechanisms of perturbation propagation have been proposed to explain sympathetic phenomena: MHD waves, fast

particle fluxes, Morton waves, sub-photospheric perturbations, etc. .

With the appearance of radio telescopes with sufficiently good spatial and temporal resolution, sympathetic phenomena began to be studied by radio astronomical methods. In [Nakajima et al., 1985], based on observations on the one-dimensional Nobeyama interferometer at the wave1.76 cm, 122 cases of sympathetic events were detected over a period of 3 years. From these, 5 events with intervals of less than 1 minute and similar temporal profiles were selected for a more detailed study. In the studied events, the distance between active regions was $(1.5\text{-}9)\times10^5$ km and the time interval between events was 1.5-25 s, giving an estimate of the perturbation propagation velocity of $(3\text{-}11)\times10^4$km/sec. High-energy electrons were assumed to be the perturbing agent. Similar phenomena have also been studied using multi-azimuth observations at RATAN-600 [Golubchina et al., 2004].

The purpose of our work is to identify and study the events that can presumably be sympathetic, by analyzing the archive of observations on the Nobeyama radioheliograph, which may further clarify the nature of sympathetic flares, as well as to better understand the mechanisms of solar flare development. The emphasis of this work is on estimating the velocity of the perturbing agent. In this paper, we consider two series of radio bursts that are likely to be sympathetic.

2. OBSERVATIONAL STUDIES

To address the objectives, we used the Nobeyama Radioheliograph (NoRH) observational archive [Nakajima et al., 1994; Hanaoka et al., 1994; Shibasaki et al., 1994] at 17 GHz (wavelength1.76 cm). NoRH is an instrument with suitable parameters for studies of sympathetic phenomena in the radio band due to the accumulated long series of daily (6-8 hours per day) observations (from 1992 to 2020), high temporal (1 sec) and spatial (10 sec arc at the1.76 см) wavelength resolution.

In this work, we used data only in the intensity channel (Stokes parameter I). Radio images of the full disk of the Sun were synthesized for the entire day of observations (about 8 hours) with an interval of 10 s and an averaging time of 10 s. The spatial resolution of the NoRH at 17 GHz is about 10-20 sec of arc, depending on the height of the Sun. The spatial resolution of the NoRH at 17 GHz is about 10-20 sec of arc, depending on the Sun's altitude. Then, time profiles of the maximum brightness temperatures of the studied ARs were constructed. For this purpose, the field-of-view (FOV) in which the studied AO fell in each image was selected and the maximum brightness temperature in the FOV was calculated. To be sure that we were plotting a profile of the same region, we simultaneously plotted and analyzed the time profiles of the coordinates of the maximum luminance temperature points at the same time as the time profile of the maximum luminance temperature.

From the delay time between the initiating and initiating bursts, an estimate of the velocity of

the perturbing agent was made. This raises two questions: how to measure the delay and how to measure the distance. The propagation trajectory of the perturbing agent is unknown. Therefore, it was necessary to make assumptions about its possible propagation trajectories. As an estimate of the distance between AOs, we took the arc length of a large circle on the photosphere passing through the AOs under study. As an estimate of the perturbation propagation time, we took the time interval between the moment of the maximum of the initiating burst and the moment of the beginning of the initiated burst. Obviously, such an estimate is rather coarse. The error can reach 50% or more. But, nevertheless, it gives an idea of the order of magnitude of the perturbation propagation.

In the present paper we consider two sympathetic events: September 112001 г . and June 302003 г . In the first case, two sympathetic events occurred in a day, while in the second case, three sympathetic events occurred in a day.

Figure 1a shows the radio image of the Sun at 17 GHz from observations at NoRH before the flares. White squares indicate the four field-of-view (FOV) regions for which the time profiles of the maximum brightness temperatures were plotted. Two of them (FOV1 and FOV4) are located in AR NOAA 9608. FOV2 is located in AR NOAA 9605, and FOV3 is located in AR NOAA 9601.

The first initiating burst occurs in FOV1 at approximately 0:59 UT. Its position is indicated by the arrow in Fig. 1b. Then, after about 2 minutes, a burst occurs in FOV2 (Fig. 1c), and after about another two minutes a burst in FOV3 (Fig. 1d). The corresponding time profiles are shown in Fig. 2. For this event, we made an estimate of the perturbing agent's velocity in two ways. First - we first estimated the perturbation transmission rate from burst 1 to burst 2, then from burst 2 to 3, assuming that burst 2 in FOV2 is the initiating burst in this case. Second, we estimated the perturbation transfer rate from burst 1 to burst 3. The results are summarized in Table.

The second initiating burst occurs in FOV4 at about 1:58 UT. We have labeled it with the number 4. The corresponding initiating burst, labeled by number 5, occurs about 2 min later in FOV2 (Fig. 3b). Fig. 4 shows the corresponding time profiles. The estimated velocity of the perturbing agent is summarized in Table.

Figs. 5 and 6 show the sympathetic outbursts that occurred on June 30 2003г . Fig. 5a shows a white-light image of the Sun from SOHO/MDI data, and Fig. 5b is a radio image at 17 GHz from NoRH data. The initiating bursts occurred in AR NOAA 10396 and the secondary bursts occurred in AR NOAA 10397. In Fig. 6 we present the time profiles of the maximum brightness temperatures of these ARs derived from the radio maps. The plots clearly show 3 pairs of bursts, and even a correlation of the maximum values of the bursts is observed: the higher the maximum temperature of the initiating burst, the higher the temperature of the secondary burst. AO 10397 shows a burst (about $4^{h)}$ that has no initiating burst, but perhaps the processes that occurred in AO

10397 from $2^{(h)}30^{m}$to $4^{h}$are a single response to the second burst in AO 10396.

Three cases of sympathetic events during the observation series of 8 hours duration suggest that these coincidences are not accidental and there was a real physical connection between AOs 10396 and 10397. NOAA AOs 10396 and 10397 were more than 90 degrees apart in solar longitude. The outbursts in these regions occurred with a delay of 10 to 20 min, indicating a significant magnitude of the propagation velocity of the perturbing agent, estimates of which are summarized in the Table. The Table shows that, taking into account the rather large error in the velocity estimates, in both cases considered, the perturbation transmission rates from one to the other AO were approximately the same.

3. CONCLUSIONS

We have thus considered two series of sympathetic events: two pairs of bursts on September 11, 2001 and three pairs of bursts on June 30, 2003. In both cases considered, we obtained approximately the same estimates of the perturbation transmission velocities from one AO to the other, which are 1000-5000 km/sec.

Since we have analyzed a small fraction of the solar observational archive at NoRH, we can assume that sympathetic phenomena in the radio band are not exotic events and have been observed quite often. The solar observational archive accumulated at NoRH, containing a long series of daily observations with good spatial and temporal resolution, is well suited for the study of sympathetic phenomena in the radio band, and the potential of this archive is far from being exhausted. For future studies of sympathetic outbursts in the radio band, it seems appropriate to also use the observations from the Siberian Radioheliograph and SDO/AIA.

ACKNOWLEDGEMENTS

This work was performed using data from the Nobeyama radioheliograph. The author is grateful to the reviewers for their helpful suggestions.

FUNDING

The work was carried out under the State assignment.

CONFLICT OF INTERESTS

The author declares that he has no conflict of interest.

REFERENCES

1. *Lebedev N.I., Lebedev M.N., Ishkov V.N.* Probable sympathetic outbursts of the year of the maximum of the current 25th solar activity cycle // The twentieth conference "Plasma Physics in the Solar System". February 10-14, 2025, ICI RAS. Abstracts of reports. p. 81. 2025.

2. *Fritzova-Svestkova L., Chase R. C., Svestka Z.* On the occurrence of sympathetic flares // Solar Physics. V. 48. P. 275-286. 1976.
3. *Golubchina O.A., Tokhchukova S.K., Bogod V.M., et al.* Synchronous Microwave Brightenings of Solar Active Regions from RATAN-600 Spectral Observations // Astronomy Letters. V. 30. N 10. P. 715-727. 2004.
4. *Hanaoka Y., Shibasaki K., Nishio M., et al.* Processing of the Nobeyama Radioheliograph Data // In: Proceedings of Kofu Symposium, Kofu, Japan, Sept. 6-10, 1993. P. 35-43. 1994.
5. *Nakajima H., Dennis B. R., Hoyng P., et al.* Microwave and X-ray observations of delayed brightenings at sites remote from the primary flare locations // The Astrophysical Journal. V. 288. P. 806-819. 1985.
6. *Nakajima H., Nishio M., Enome S., et al.* The Nobeyama radioheliograph // IEEE Proceedings. V. 82. P. 705-713. 1994.
7. *Richardson, R.S.* // Ann. Rep. Director Mt. Wilson Obs. V. 35. P. 871. 1936.
8. *Richardson R.S.* Characteristics of Solar Flares // The Astrophysical Journal. V. 114. P. 356-367. 1951.
9. *Shibasaki K., Enome S., Nakajima H., et al.* The Nobeyama Radioheliograph Data Use // In: Proceedings of Kofu Symposium, Kofu, Japan, Sept. 6-10, 1993. P. 45-51. 1994.
10. *Wang H., Chae J., Yurchyshyn V., et al.* Inter-Active Region Connection of Sympathetic Flaring on 2000 February 17 // The Astrophysical Journal. V. 559. N 2. P. 1171-1179. 2001.
11. *Wheatland M. S., Craig I.J.D.* Including Flare Sympathy in a Model for Solar Flare Statistics // Solar Physics. V. 238. N 1. P. 73-86. 2006.

Table. Events considered.

Date	Time	Primary outburst	Secondary surge	V km/sec
2001-Sep-11	00:59	9608, 1	9605, 2	2900
2001-Sep-11	00:59	9608, 2	9601, 3	4500
2001-Sep-11	00:59	9608, 1	9601, 3	3800
2001-Sep-11	01:59	9608, 4	9605, 5	2300
2003-Jun-30	00:15	10396	10397	3800
2003-Jun-30	02:30	10396	10397	3900
2003-Jun-30	05:30	10396	10397	1100

Notes to the Table.

The Time column gives the starting moments of the events, Primary burst is the number of the AO in which the initiating radio burst occurred, for September 112001 г . the burst numbers from Figures 2 and 4 are given, Secondary burst is the number of the AO in which the secondary radio burst occurred, V is an estimate of the velocity of the perturbing agent.

FIGURE CAPTIONS

Fig. 1. Radio images of the Sun at 17 GHz from observations at NoRH on September 11, 2001 for the first pair of sympathetic events (bursts 1, 2, and 3 in Fig. 2).

(a) Radio images at the moment before the bursts. The image shows the regions (field-of-view, FOV) where the time profiles of the maximum brightness temperatures were plotted.

(b) Radio image at the time of the initiating outburst, labeled in Fig. 2 with number 1. It can be seen that there are no prominent radio sources in AOs 9605 and 9601.

c). Radio image at the time of the secondary burst in AO 9605, denoted in Fig. 2 by numeral 2. The source is shown with an arrow. There is no bright source in AO 9601.

d). Radio image at the time of the secondary burst in AO 9601, denoted in Fig. 2 by numeral 3. The source is shown with an arrow.

Fig. 2. Time profiles of the maximum brightness temperatures of the radio emission on September 11, 2001 plotted for AO 9608 (FOV1), 9605 (FOV2), and 9601 (FOV3) for the first event at 0:59. Panel a) shows a general view of the time profiles, panel b) shows the sympathetic bursts on a large scale. A slight vertical shift has been added to prevent the curves from overlapping.

Fig. 3. Radio images of the Sun at 17 GHz from observations at NoRH on September 11, 2001 for the second pair of sympathetic events (bursts 4 and 5 in Fig. 4). Panel a) shows the image before the bursts, panel b) shows the image during the bursts. The arrows indicate the sources of the bursts.

Fig. 4. Time profiles of the maximum brightness temperatures of the radio emission on September 11, 2001 plotted for AO 9608 (FOV4) and 9605 (FOV2) for the second event at 1:59. Panel a) shows a general view of the time profiles, panel b) shows the sympathetic bursts on a large scale.

Fig. 5.a) White-light image of the Sun from SOHO/MDI data on June 30, 2003, (b) - 17 GHz radio image from NoRH data on June 30 .2003 г

Fig. 6. Time profiles of maximum microwave brightness temperatures (17 GHz) of NOAA AOs 10396 and 10397 from NoRH data on June 30, 2003. The abscissa axis is the UT time, 0 corresponds to 00:00 UT on June 30, 2003, the ordinate axis is the maximum brightness temperatures of the AOs.

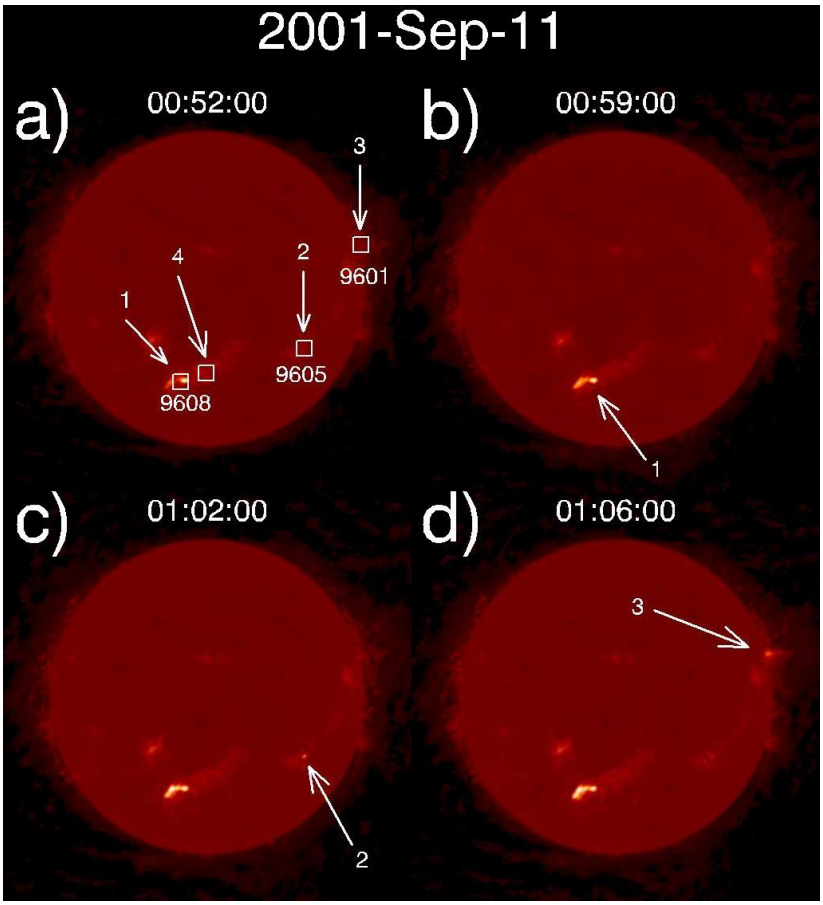
2001-Sep-11
a)
00:52:00
b)
00:59:00
c)
01:02:00
d)
01:06:00
1
2
3
4
9601
9605
9608

Fig. 1.

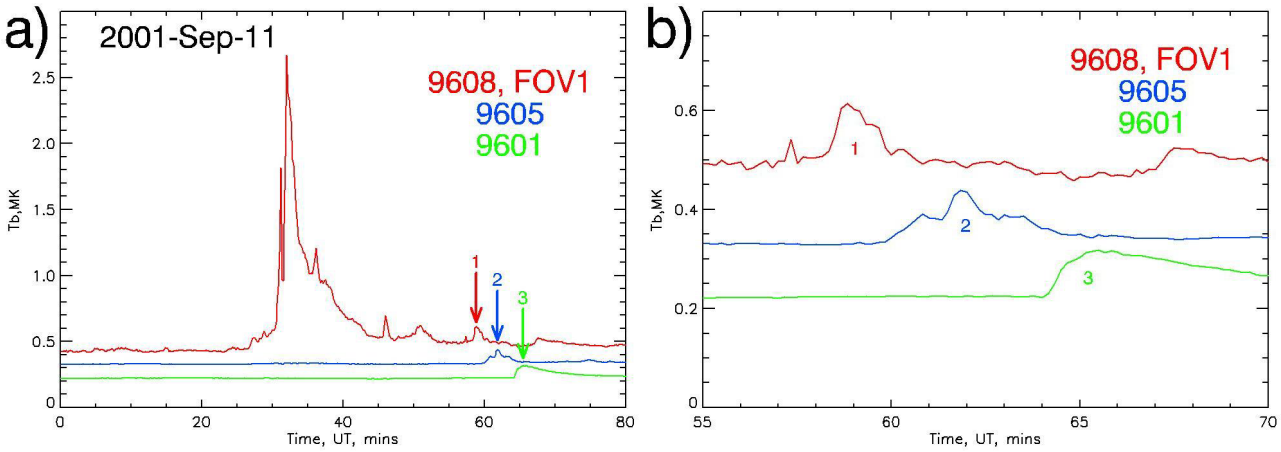
a)
2001-Sep-11
9608, FOV1
9605
9601
Tb,MK
Time, UT, mins
b)
9608, FOV1
9605
9601
Tb,MK
Time, UT, mins

Fig. 2.

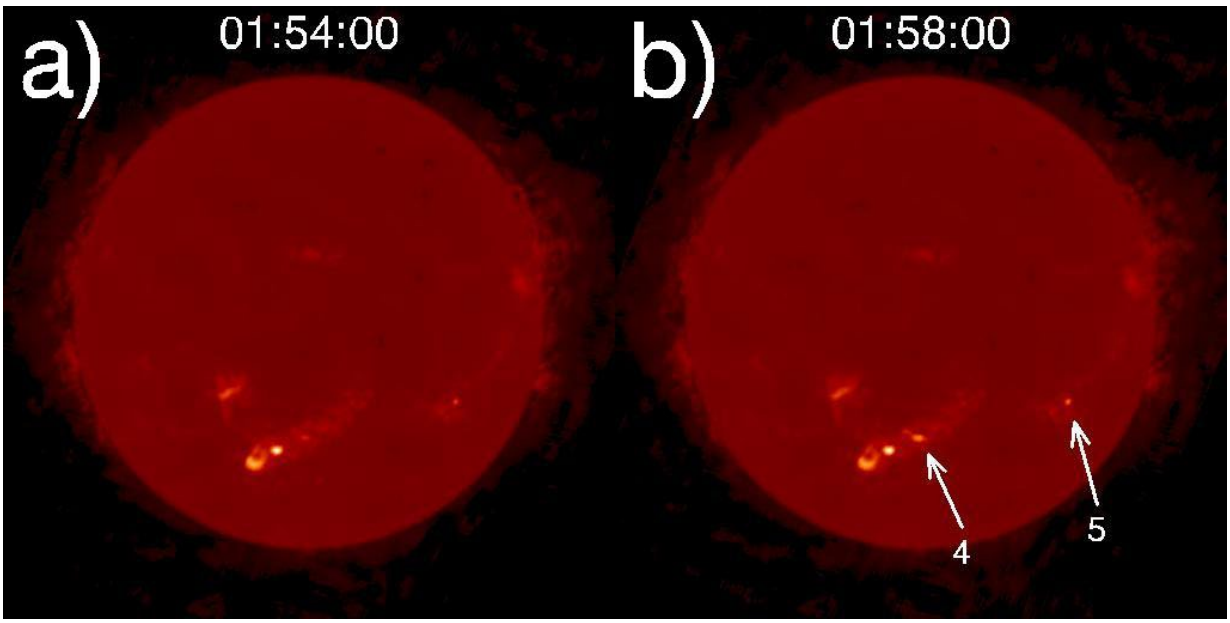
a)
01:54:00
b)
01:58:00
4
5

Fig. 3.

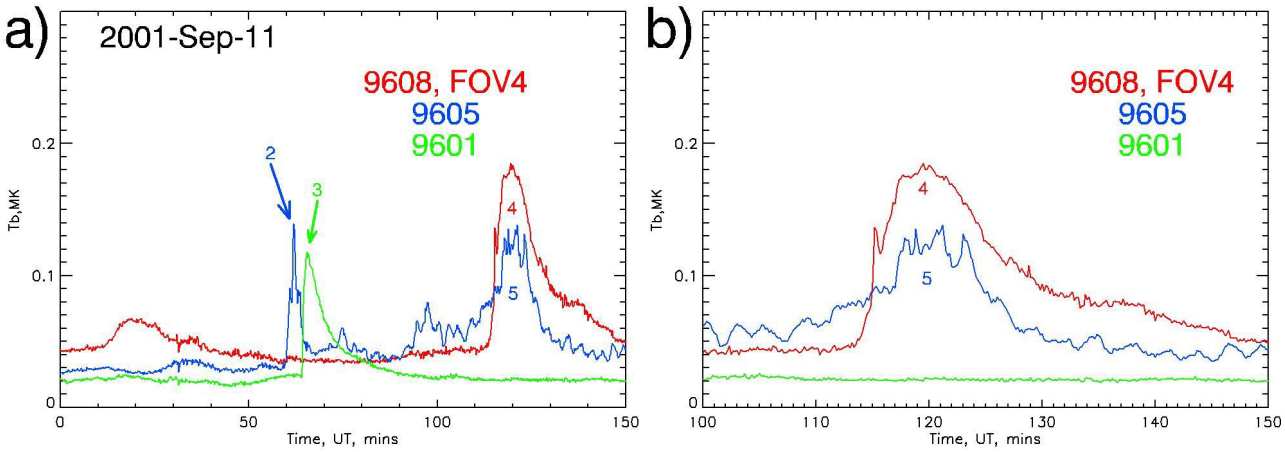
a)
2001-Sep-11
9608, FOV4
9605
9601
2
3
4
5
Tb,MK
0
0.1
0.2
0
50
100
150
Time, UT, mins
b)
9608, FOV4
9605
9601
4
5
Tb,MK
0
0.1
0.2
100
110
120
130
140
150
Time, UT, mins

Fig. 4.

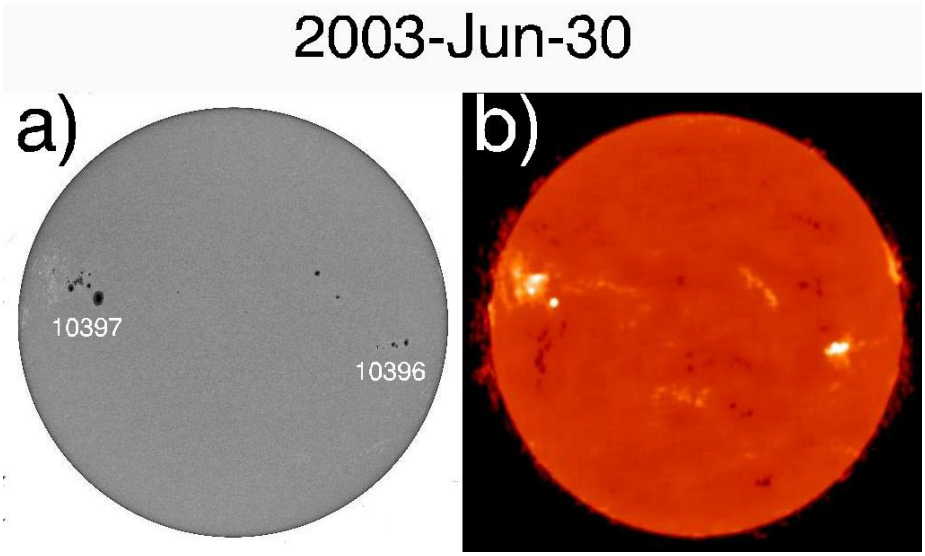
2003-Jun-30
a)
b)
10397
10396

Fig. 5.

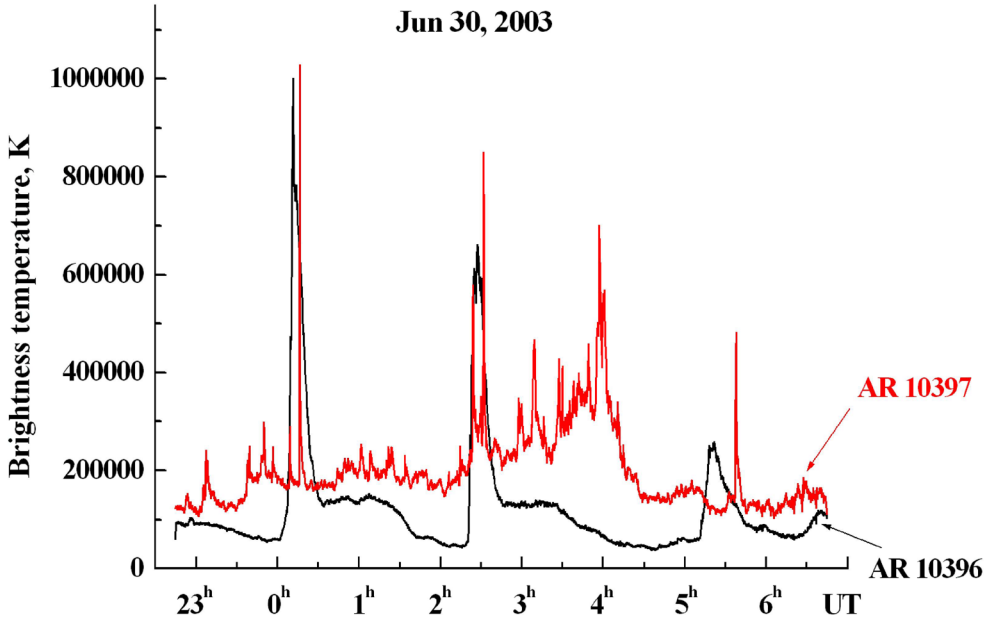
Jun 30, 2003
Brightness temperature, K
1000000
800000
600000
400000
200000
0
AR 10397
AR 10396
23h
0h
1h
2h
3h
4h
5h
6h
UT

Fig. 6.